EUROPEAN ORGANIZATION FOR NUCLEAR RESEARCH

Letter of Intent to the ISOLDE and Neutron Time-of-Flight Committee

Production test of Ti isotopes towards laser spectroscopy experiments

April 19, 2023

P. Plattner[1], S. Bai[2], K. Blaum[1], B. Cheal[3], R. F. García Ruíz[4], P. Imgram[5], K. Koenig[6], T. Lellinger[6,7], K. Minamisono[8], P. Müller[6], W. Nazarewicz[8], R. Neugart[1,9], G. Neyens[5], W. Nörtershäuser[6], P.G. Reinhard[10], R. Sánchez[11], L. Renth[6], L. V. Rodríguez[1], X. F. Yang[2], D. T. Yordanov[12]

[1] *Max-Planck-Institut für Kernphysik, Heidelberg, Germany*
[2] *School of Physics and State Key Laboratory of Nuclear Physics and Technology, Peking University, Beijing, China*
[3] *Oliver Lodge Laboratory, University of Liverpool, UK*
[4] *Massachusetts Institute of Technology, Cambridge, MA, USA*
[5] *Instituut voor Kern- en Stralingsfysica, KU Leuven, Leuven, Belgium*
[6] *Institut für Kernphysik, Technische Universität Darmstadt, Darmstadt, Germany*
[7] *Experimental Physics Department, CERN, Geneva, Switzerland*
[8] *Michigan State University, East Lansing, MI, USA*
[9] *Institut für Kernchemie, Universität Mainz, Mainz, Germany*
[10] *Friedrich-Alexander-Universität, Erlangen-Nürnberg, Germany*
[11] *GSI Helmholtzzentrum für Schwerionenforschung GmbH, Darmstadt, Germany*
[12] *Université Paris-Saclay, CNRS/IN2P3, IJCLab, 91405 Orsay, France*

Spokesperson: Peter Plattner, peter.plattner@cern.ch
Contact person: Peter Plattner, peter.plattner@cern.ch

Abstract: The titanium isotopic chain is of significant interest due to its close relationship with calcium and proximity to the $N=20$, 28, and 32 shell closures. The results of an investigation of the titanium chain would offer important insights into the nuclear structure and properties of titanium and their relationship with calcium and argon, which can contribute to a better understanding of the behavior of these elements and their isotopes. At this moment the yields of titanium isotopes at ISOLDE seem unclear, hence an investigation of the yields of radioactive titanium is necessary to determine the extent of accessibility of titanium isotopes for collinear laser spectroscopy.

Requested shifts: 9 shifts, (split into 1 run over 1 year)

1 Physics Motivation

Collinear Laser Spectroscopy (CLS) plays an important role in the study of short-lived radionuclides as it reveals nuclear ground state properties such as spin, electro-magnetic moments and mean-square nuclear charge radii [1, 2]. Thus, the technique of CLS improves our understanding of nuclear structure and its peculiarities, such as the magicity of certain proton and neutron numbers. One important unanswered question is if magic numbered isotopes, i.e. nuclei with enhanced stability, are universal and if the appearance and disappearance of such magic numbers, as seen in the appearance of $N=16$ in oxygen and the disappearance of $N=28$ in silicon [3–6]. In this regard the calcium region is very important due to the accessibility of numerous magic numbered isotopes, namely $Z=20$, $N=20$, $N=28$ and $N=32$.

To further our understanding of the structure of magic calcium several CLS experiments have been performed in the past, such as for the $Z=19$ potassium [7], the $Z=20$ calcium [8] and the $Z=21$ scandium [9] chains, with current efforts at COLLAPS to push towards CLS measurements of calcium up to and beyond $N=32$ with the ROC technique. In this regard the $Z=22$ titanium chain, as the next in line after scandium, offers further insights into nuclear structure in this region.

1.1 Investigation of Mean Square Charge Radii

In particular, nuclear charge radii can be used to benchmark nuclear models. To prove their accuracy, the distinctive kink at neutron shell closures has to be replicated by these models. The nuclear charge radii of stable isotopes of titanium $^{46\text{-}50}$Ti up to the neutron shell closure at $N=28$ have been investigated exhaustively in the past through a variety of methods [10–14], including CLS measurements of neutron-deficient ^{44,45}Ti at IGISOL [15]. To further study nuclear models and their ability to reproduce charge radii and kinks of different elements in this region, at least two more isotopes above the $N=28$ shell closure are necessary.

Moreover, measured charge radii of titanium across the $N=28$ shell closure can also act as a test bed for the calibration of mass and field-shift factors. Considering that several elements in this region only exhibit a single stable isotope, such as scandium, vanadium, manganese or cobalt, the mass and field shift factors have to be calculated through atomic theory, which usually suffers from large uncertainties. It has been noted that the increase in differential mean square charge radii relative to $N=28$ seem largely independent of the proton number in this region for N≥28 [16] (compare also fig. 1, left). As such, this has been used to determine the degree of uncertainty on the mass shift factor for the manganese chain in the past [17]. Titanium, with its five stable isotopes, will provide another independent case to further test atomic theory by comparing the field and mass-shift with those obtained from King plot analysis. Consequently, for future measurements of isotopic chains like scandium or vanadium, where King plot analysis is not possible, our confidence in the slope beyond $N=28$ will be reinforced.

Towards neutron-deficient isotopes, the $N=20$ shell closure does not exhibit the usual kink behaviour for the potassium and calcium chains (see fig. 1, left). However, recent results from the BECOLA group have shown the appearance of a kink in the charge radii

of scandium isotopes across the shell closure [18]. As such it is of broad interest whether a similar kink appears in the titanium chain.
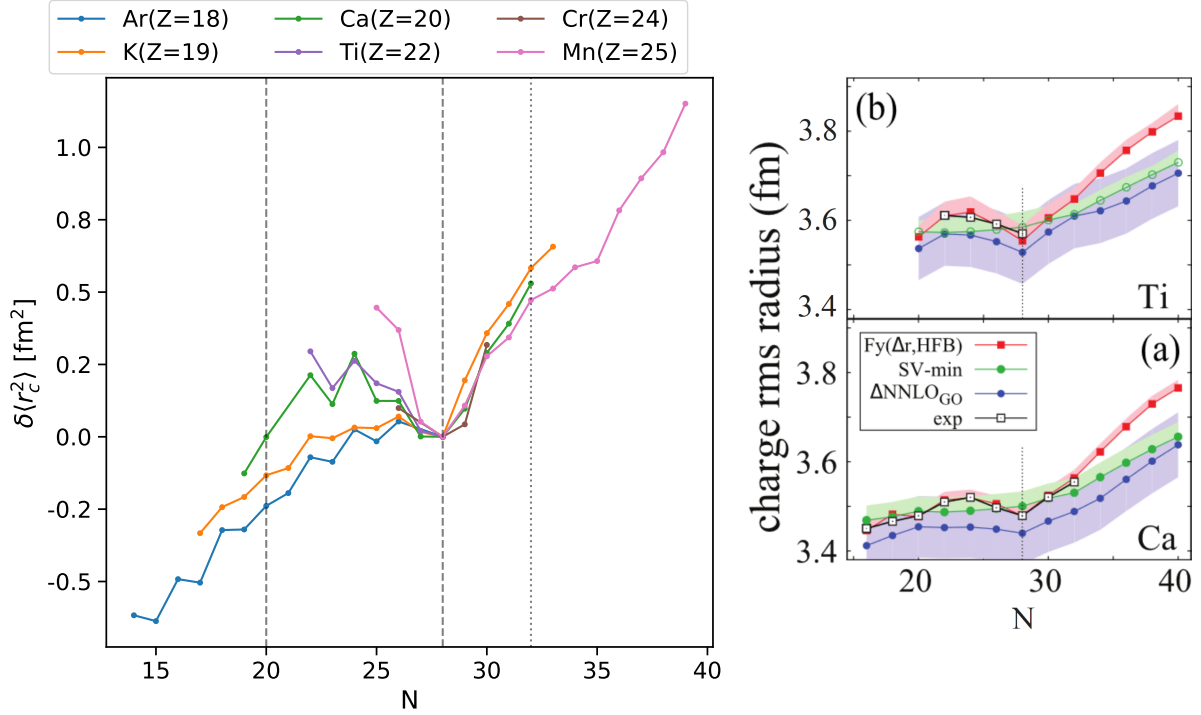

Figure 1: Left: Difference in mean square charge radius to $N=28$ of of argon, potassium, calcium, titanium, chromium and manganese. For clarity the uncertainties were omitted. Values taken from [7, 8, 19–21]. Right: Theory prediction of DFT and coupled cluster calculations for absolute charge radii of calcium and titanium. Figure adapted from [22].

In addition, the remarkable resemblance in the change in mean square charge radius between $N=20$, and $N=28$ in calcium and titanium presents an intriguing research opportunity. In fact, coupled cluster and Fayans' density functional theory calculations predict that the root mean square charge radii of titanium at $N=20$ and $N=28$ should be almost equal [22], similar to the charge radii of calcium (see also fig. 1, right). From the known experimental data it is obvious that the trend of charge radii for calcium and titanium are very similar, but the charge radii towards $N=20$ for titanium are missing at this moment. Therefore, it is imperative to investigate whether this pattern persists or whether the charge radii increase further towards the $N=20$ shell closure by measuring the charge radii of ^{42,43}Ti.

Conversely, shell closure effects in $N=32$ seem to be a contentious topic in literature. For example, potassium does not exhibit a kink in charge radii [7] but there are clear indications of strong shell-like behaviour from mass measurements in the two-neutron separation energy S_{2n} and the empirical neutron-shell gap Δ_{2n} for the potassium, calcium and scandium chains [23]. This shell-like behaviour of Δ_{2n} weakens in the titanium chain and completely disappears for the vanadium chain, indicating a quenched shell [23]. Therefore, measurements of charge radii in this region would further constrain nuclear models and provide valuable benchmarks in this important region of the nuclear chart.

The goal of this letter of intent is to evaluate for which titanium isotopes the ISOLDE production rates are sufficient to carry out CLS. Further interest for titanium isotopes comes from the experimental determination of nuclear moments.

1.2 Investigation of Nuclear Moments

The region between $N=20$ and $N=28$ is intriguing for the investigation of nuclear structure due to the unique $f_{7/2}$ orbital within the shell, as this is a prime example for the single particle character of neutrons above the $N=20$ filled shell. Moments of such nuclei allow the characterisation of residual nucleon-nucleon interaction, which were established empirically in the past [24]. In titanium most of the odd numbered isotopes between $N=20$ and $N=28$ exhibit an $I=7/2$ ground state, with the exception of ^{47}Ti with $I=5/2$. This is similar to the ^{43}Ar isotone that also exhibits an $I=5/2$ ground state with a close lying $I=7/2$ isomeric state, which could be explained as an anomalously coupled $(f_{7/2}^5)_{5/2}$ configuration [25].
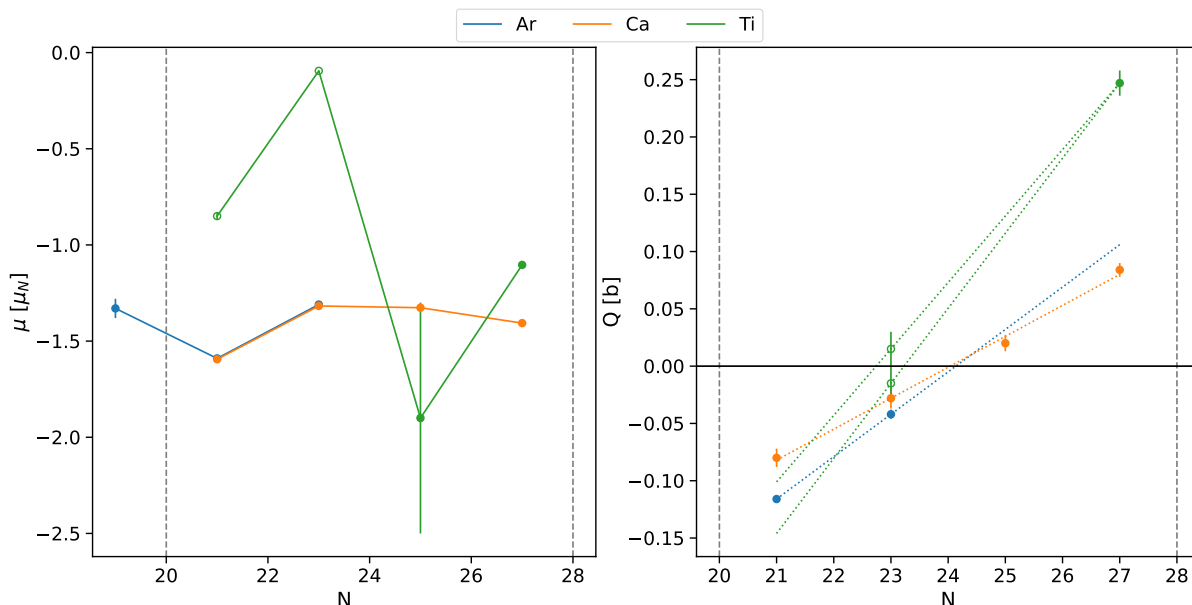

Figure 2: Magnetic moments (left) and quadrupole moments (right) of $I=7/2^-$ states of argon, calcium and titanium. Empty circles were used in case the sign was not known and it had to be presumed. Data from [26, 27].

When comparing the closed calcium core with two additional protons of titanium with the calcium core with two proton holes of the argon chain we find that the known magnetic moments of ^{39,41}Ar and ^{41,43}Ca are identical within the experimental uncertainties (see fig. 2). The known moments from atomic beam magnetic resonance spectroscopy [28], with presumed signs, for the corresponding ^{43,45}Ti are quite different. All present measurements stem from different techniques which could result in different systematic uncertainties. As such, an investigation of all possible $I=7/2^-$ isotopes, with the same experimental technique could provide interesting findings.

4

Table 1: List of titanium nuclides with currently measured magnetic dipole, electric quadrupole moments and nuclear charge radii, accessible by collinear laser spectroscopy. Data from [21, 29, 30].

A	I^π	$\tau_{1/2}$		$\mu[\mu_N]$	Q_s [b]	$\sqrt{\langle r^2 \rangle}$ [fm]
42	0^+	208.7	ms			
43	$7/2^-$	509.0	ms	$\pm 0.85(2)$		
44	0^+	59.1	a			3.6115(51)
45	$7/2^-$	3.1	h	$\pm 0.095(2)$	$\pm 0.015(15)$	3.5939(32)
46	0^+	stable				3.6070(22)
47	$5/2^-$	stable		$-0.788\,48(1)$	$+0.302(10)$	3.5962(19)
48	0^+	stable				3.5921(17)
49	$7/2^-$	stable		$-1.104\,17(1)$	$+0.247(11)$	3.5733(21)
50	0^+	stable				3.5704(22)
51	$3/2^-$	5.8	min			
52	0^+	1.7	min			
53	$(3/2)^-$	32.7	s			
54	0^+	2.1	s			
55	$(1/2)^-$	1.3	s			
56	0^+	200.0	ms			

Additionally, the absolute magnetic moment for ^{45}Ti of $|\mu|=0.095(2)\,\mu_N$ is about one order of magnitude smaller, when comparing to other isotopes with spin $7/2^-$ (see table 1). Furthermore, the absolute magnetic moment is also far smaller than for the $I=7/2^-$ isobar ^{45}Ca with $\mu=-1.3274(14)\,\mu_N$. This highly anomalous value should be further investigated.

The single-particle shell model predicts a linear trend of the quadrupole moments across a single-orbit shell, with the quadrupole moment of a single particle being equal but opposite sign to that of a single hole and a zero crossing in the middle of the shell. This is demonstrated very well in the calcium chain and to a lesser degree in the trend of the argon chain (see fig. 2). When comparing with titanium we find a shifted zero crossing regardless of the actual sign of the quadrupole moment of ^{45}Ti. On top of this, the expected value, when applying the single-particle shell model for the quadrupole moment of ^{43}Ti, is supposed to be far lower than for argon and calcium at $N=21$, which is not supported by the current trend of known quadrupole moments in the titanium chain.

2 Laser Spectroscopy

The HRS target could be used to produce isotopes of titanium, that can be ionised using a previously tested RILIS scheme. Use of the HRS target station permits access to ISCOOL cooler-buncher to provide bunched beams for the COLLAPS CLS setup. At COLLAPS the ions will be collinearly overlapped with a continuous-wave laser beam. The observed frequency in the ion's rest frame can be tuned by changing the voltage of the Doppler-tuning electrodes before COLLAPS' optical detection region. As consequence, the ions' hyperfine transitions can be resonantly excited and the fluorescence signal from

de-excitation can be recorded. Time gates can be applied to the fluorescence signal, due to the bunched beam, to reduce the photon background by several orders of magnitude. For further details on the experimental setup, we refer to [2].

While Due to the $\sim$100 ms accumulation time in the cooler-buncher, the extracted ions are expected to mostly populate the ionic ground state. Titanium exhibits several strong lines from the ionic ground state, in the region between 300 nm and 350 nm, accessible by frequency-doubled dye lasers. Of particular note are the $3d^2 4s\ ^4F_{3/2} \to 3d^2 4p\ ^4G_{5/2}$ (338.47 nm, A=$1.39 \times 10^8\,\text{s}^{-1}$), $3d^2 4s\ ^4F_{3/2} \to 3d^2 4p\ ^4F_{3/2}$ (324.29 nm, A=$1.47 \times 10^8\,\text{s}^{-1}$) and $3d^2 4s\ ^4F_{3/2} \to 3d^2 4p\ ^4D_{1/2}$ (307.72 nm, A=$1.71 \times 10^8\,\text{s}^{-1}$) lines. All three transitions exhibit high Einstein coefficients with lifetimes of the excited states around 6 ns and branching ratios to the ionic ground state from 60.2 % to 79.3 %. Thus, several resonant excitations per ion are possible.

For titanium, an ionic transition is preferred over an atomic one, mainly because the charge exchange process leads to a significant division of populated states [31]. Additionally, the limited knowledge we have of the transition strengths of these states makes the ionic transition a more viable option. For our experiment we plan to use the 338.47 nm transition, due to its sensitivity to the magnetic dipole and electric quadrupole moments. Furthermore, this transition has been tested previously at TU Darmstadt and exhibits a splitting that is large enough to resolve all individual hyperfine transitions for the odd-numbered isotopes [32].

3 Predicted Yields

The ISOLDE yield database only shows a single measurement, using the PSB as a driver with a UC_x target, of 7 ions/µC. As titanium is expected to also form titanium carbide, this single predicted yield is expected to be of lower value than possible for other target materials. To estimate yields ABRABLA simulations have been performed, which indicate similar in-target production for UC_x and tantalum targets (see fig. 3, left).

Furthermore, estimates from ISOLTRAP during a TISD, including a RILIS scheme for titanium, provide yields between 1.5×10^5 ions/µC to 1.85×10^6 ions/µC for the stable ^{46,48,50}Ti isotopes with an estimated RILIS improvement of a factor of 1200. A second yield estimate, obtained during a scandium TISD with a tantalum target, provides a surface ionisation yield for ^{50}Ti of $\geq 2.5 \times 10^6$ ions/µC. This yield, solely from surface ionisation of titanium from a Ta-foil target, is already far higher than the previously obtained yield from the UC_x target, using RILIS. Thus, it is expected that the Ta-foil target with RILIS should achieve orders of magnitude higher yields (see fig. 3, right).

Currently there is little information about the yields of radioactive titanium isotopes, although preliminary numbers, obtained from yield measurements at ISOLTRAP, suggest a large improvement when using a tantalum foil target instead of uranium carbide. For this reason, we propose to systematically determine the production yields of titanium nuclides, using RILIS and a non-UC_x target, which will allow to determine the extent of accessibility of $^{42\text{-}45,51\text{-}55}$Ti nuclides using the COLLAPS experiment.

Summary of requested shifts: 9 shifts (1 shift per radioactive isotope).
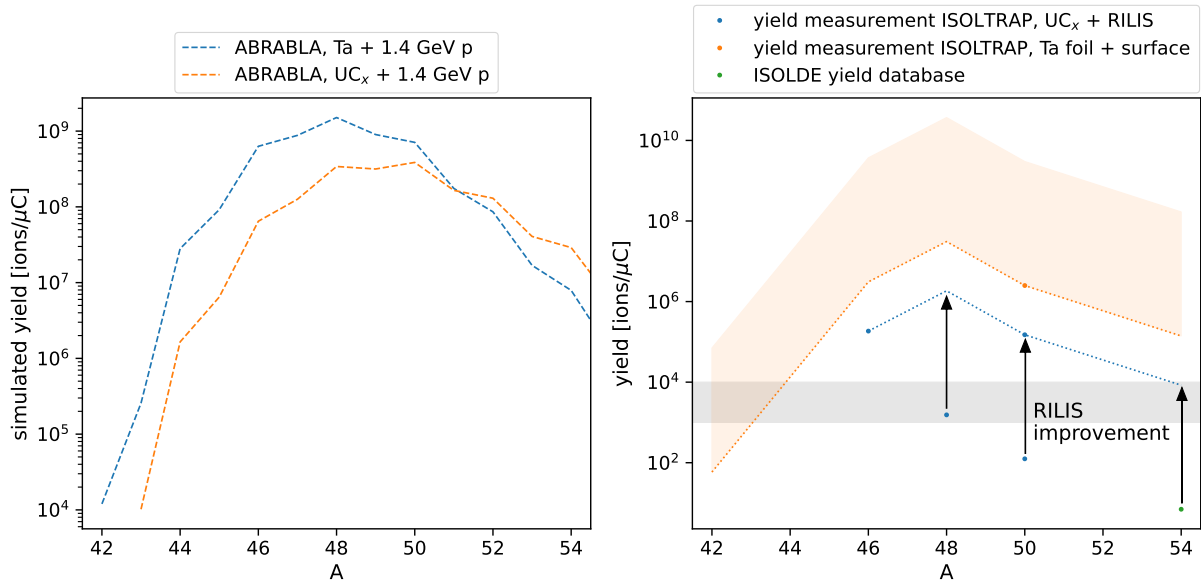
Figure 3: Left: ISOLDE yields simulated using ABRABLA with tantalum foil and UC_x targets and 1.4 GeV protons. Right: yield estimates provided by ISOLTRAP obtained during TISD for titanium and scandium and value from ISOLDE yield database for ^{54}Ti, scaled by the obtained RILIS improvement factor from ISOLTRAP. Dotted lines provide estimates based on the observed trends from ISOLTRAP data and the in target production for $^{42\text{-}45}$Ti. The light shaded area indicates the possible gain by RILIS over surface ionization. COLLAPS sensitivity limit is indicated by the dark shaded area.

References

[1]   P. Campbell et al., Progress in Particle and Nuclear Physics **86**, 127–180 (2016).

[2]   R. Neugart et al., Journal of Physics G: Nuclear and Particle Physics **44**, 10.1088/1361-6471/aa6642 (2017).

[3]   A. Ozawa et al., Physical Review Letters **84**, 5493–5495 (2000).

[4]   M. Stanoiu et al., Physical Review C **69**, 034312 (2004).

[5]   B. A. Brown et al., Physical Review C **72**, 057301 (2005).

[6]   B. Bastin et al., Physical Review Letters **99**, 022503 (2007).

[7]   Ã. Koszorús et al., Nature Physics **17**, 439–443 (2021).

[8]   R. F. Garcia Ruiz et al., Nature Physics **12**, 594–598 (2016).

[9]   S. Bai et al., Physics Letters B **829**, 137064 (2022).

[10] G. Fey et al., Zeitschrift für Physik **265**, 401–403 (1973).

[11] H. D. Wohlfahrt et al., Physical Review C **23**, 533–548 (1981).

[12] A. Selig et al., Nuclear Physics A **476**, 413–447 (1988).

[13] Y. P. Gangrsky et al., Journal of Physics B: Atomic, Molecular and Optical Physics **28**, 957–964 (1995).

[14] B. Furmann et al., Zeitschrift für Physik D Atoms, Molecules and Clusters **37**, 289–294 (1996).

[15] Y. P. Gangrsky et al., Journal of Physics G: Nuclear and Particle Physics **30**, 1089–1098 (2004).

[16] K. Kreim et al., Physics Letters B **731**, 97–102 (2014).

[17] H. Heylen et al., Physical Review C **94**, 054321 (2016).

[18] K. Koenig, *private communication*, Mar. 2023.

[19] G. Fricke et al., *Nuclear Charge Radii* (Springer, 2004).

[20] M Avgoulea et al., Journal of Physics G: Nuclear and Particle Physics **38**, 025104 (2011).

[21] I. Angeli et al., Atomic Data and Nuclear Data Tables **99**, 10.1016/j.adt.2011.12.006 (2013).

[22] M. Kortelainen et al., Physical Review C **105**, L021303 (2022).

[23] E. Leistenschneider et al., Physical Review Letters **120**, 062503 (2018).

[24] T. Otsuka et al., Reviews of Modern Physics **92**, 015002 (2020).

[25] K. Blaum et al., Nuclear Physics A **799**, 30–45 (2008).

[26] T. Mertzimekis et al., Nuclear Instruments and Methods in Physics Research Section A: Accelerators, Spectrometers, Detectors and Associated Equipment **807**, 56–60 (2016).

[27] R. F. G. Ruiz et al., Physical Review C **91**, 041304 (2015).

[28] R. G. Cornwell et al., Physical Review **148**, 1157–1161 (1966).

[29] N.J. Stone, *Table of Nuclear Magnetic Dipole and Electric Quadrupole Moments*, technical report (International Atomic Energy Agency, Vienna, Apr. 2011).

[30] F. Kondev et al., Chinese Physics C **45**, 030001 (2021).

[31] A. Vernon et al., Spectrochimica Acta Part B: Atomic Spectroscopy **153**, 10.1016/j.sab.2019.02.001 (2019).

[32] T. Ratajczyk, "Isotope shift measurements in Ti+ transitions using laser-ablated and thermalized ions", PhD thesis (TU Darmstadt, Darmstadt, 2021).

DESCRIPTION OF THE PROPOSED EXPERIMENT

Please describe here below the main parts of your experimental set-up:

Part of the experiment	Design and manufacturing
If relevant, write here the name of the <u>fixed</u> installation you will be using [Name fixed/present ISOLDE installation: e.g. COLLAPS, CRIS, ISS, Miniball etc]	☒ To be used without any modification ☐ To be modified
If relevant, describe here the name of the <u>flexible/transported</u> equipment you will bring to CERN from your Institute [Part 1 of experiment/ equipment]	☐ Standard equipment supplied by a manufacturer ☐ CERN/collaboration responsible for the design and/or manufacturing
[Part 2 of experiment/ equipment]	☐ Standard equipment supplied by a manufacturer ☐ CERN/collaboration responsible for the design and/or manufacturing
[insert lines if needed]	

HAZARDS GENERATED BY THE EXPERIMENT

Additional hazard from <u>flexible or transported</u> equipment to the CERN site:

Domain	Hazards/Hazardous Activities		Description
Mechanical Safety	Pressure	☐	[pressure] [bar], [volume][l]
	Vacuum	☐	
	Machine tools	☐	
	Mechanical energy (moving parts)	☐	
	Hot/Cold surfaces	☐	
Cryogenic Safety	Cryogenic fluid	☐	[fluid] [m3]
Electrical Safety	Electrical equipment and installations	☐	[voltage] [V], [current] [A]
	High Voltage equipment	☐	[voltage] [V]
Chemical Safety	CMR (carcinogens, mutagens and toxic to reproduction)	☐	[fluid], [quantity]
	Toxic/Irritant	☐	[fluid], [quantity]
	Corrosive	☐	[fluid], [quantity]
	Oxidizing	☐	[fluid], [quantity]
	Flammable/Potentially explosive atmospheres	☐	[fluid], [quantity]
	Dangerous for the environment	☐	[fluid], [quantity]
Non-ionizing radiation Safety	Laser	☐	[laser], [class]
	UV light	☐	

	Magnetic field	☐	[magnetic field] [T]
Workplace	Excessive noise	☐	
	Working outside normal working hours	☐	
	Working at height (climbing platforms, etc.)	☐	
	Outdoor activities	☐	
Fire Safety	Ignition sources	☐	
	Combustible Materials	☐	
	Hot Work (e.g. welding, grinding)	☐	
Other hazards			